Combust. Sci. and Tech., 1993, Vol. 89, pp. 1-7
Photocopying permitted by license only

The Thickness Distribution of OH Regions in a Turbulent Diffusion Flame

A. W. JOHNSON and K. R. SREENIVASAN *Department of Mechanical Engineering, Yale University, New Haven, CT 06520, USA*
M. WINTER *United Technologies Research Center, East Hartford, CT 06108, USA*

(Received August 19, 1991; in final form June 12, 1992)

Abstract—The OH radicals in a hydrogen diffusion flame burning in ambient air were visualized using planar laser-induced fluorescence. Local thicknesses of the OH regions were measured at three downstream distances. Measurements show that the thickness is distributed approximately according to a lognormal probability density function.

1. INTRODUCTION

The spatial structure of turbulence plays a significant role in determining dynamical processes such as mixing, stability, and lift-off in turbulent flames. Understanding the basic structure of turbulent diffusion flames involves many issues such as turbulent mixing, scalar diffusion, multistep chemical kinetics and heat release. Molecular mixing occurs across scalar interfaces between the fuel and the oxidant. Combustion occurs when mixing is completed to stoichiometric limits within these interfaces. The corresponding heat release will in turn have a large effect on the local structure of turbulence. This interplay is quite complex, and we shall not be concerned here with those details. Instead, we concentrate on one aspect, namely the thickness distribution of hydroxyl radical (OH) in a hydrogen-air diffusion flame. OH is a product of combustion and, with some limitations to be discussed later, is considered to be a diagnostic of the flame zone.

The spatial structure of OH regions has previously been characterized in terms of thickness, axial scale, orientation, and location in hydrogen-air diffusion flames at various Reynolds numbers (Seitzman et al., 1990). However, the probability density function representing the thickness of OH regions has not previously been studied in detail. In cold flows, the thickness of mixing interfaces is on the order of the smallest scales of motion (LaRue & Libby, 1974; Sreenivasan et al., 1989). It can further be shown that the probability distribution of such scales is lognormal. If reaction zone structures have similar properties, it is possible that our knowledge of the cold flow structure may be translated, even if in a somewhat limited sense, to the characterization of combusting systems.

With this in mind, we have made measurements of the thickness distribution of the OH regions in a low-to-moderate Reynolds number hydrogen diffusion flame burning in air. The measurements show that the OH regions are quite fat (in comparison with the Kolmogorov thickness of the cold flow), and that their thickness is approximately lognormal in distribution. Some remarks are made on the interpretation of these observations.

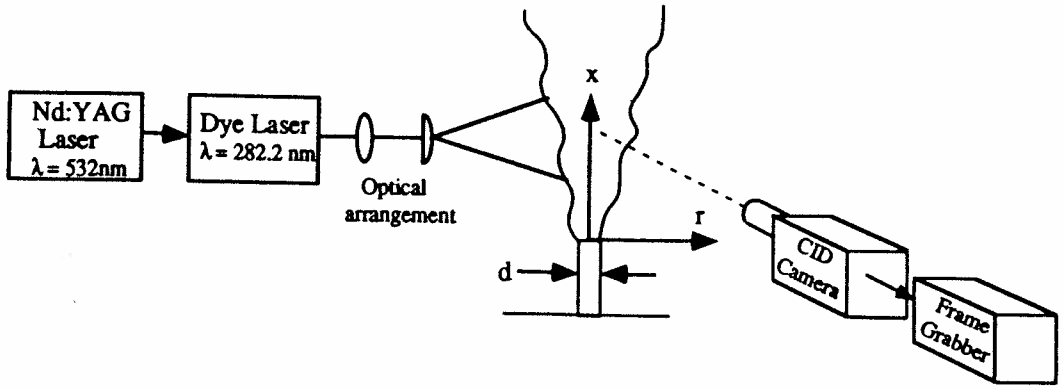

FIGURE 1. Experimental configuration for the measurement of OH radicals in a nonpremixed hydrogen flame. Nd: YAG Laser pulsed at 10 Hz. Dye Laser frequency doubled to $\lambda = 282$ nm. The CID camera had a capacity of 512 × 512 pixels and the overall resolution was about 0.1 mm/pixel. Laser sheet thickness was on the order of 0.1 mm. Nozzle diameter d = 2.5mm. The nozzle Reynolds number was Re = 2400.

mark areas where combustion has been completed—were recorded. The applicability of OH as a marker of reaction regions in flames has been discussed by Hanson (1987) and Vandsburger et al. (1988), and is also addressed later in this paper.

The experimental set up is shown in Figure 1. Hydrogen was ejected upwards from a 2.5 mm diameter round nozzle into ambient air with a nozzle velocity of 108 m/s. The cold flow Reynolds number based on nozzle diameter was Re = 2400. Images were recorded at axial positions centered around distances of 38, 58 and 98 nozzle diameters. Some details are given below.

The OH free radicals from the products of hydrogen-air reaction were visualized by planar laser-induced fluorescence (PLIF). A Spectra-Physics Nd:YAG laser frequency-doubled to a wavelength of 532 nm pumped a dye laser which was frequency-doubled to a peak absorption wavelength of OH atoms at 282 nm. The dye laser beam was passed through an optical arrangement which produced a laser sheet of thickness of the order of 100 μm. The laser pulse width was on the order of 10 nsec and the laser energy at the flame was on the order of 20-30 mJ. Fluorescence of the OH radicals were induced by the energy and wavelength of the laser sheet where the (1,0) band of the $A^2\Sigma^+$-$X^2\Pi_i$ transition was excited at 282 nm. This gives fluorescence from both (1,1) and (0,0) bands. Temperature and quenching effects on OH fluorescence were minimized by adjusting the laser to saturate the transition. Pfefferle et al. (1988) have demonstrated the effectiveness of such a technique in the PLIF images of OH in a chemically reacting boundary layer. In their work, saturation was achieved to within 10%. Illuminated regions were recorded on an intensified XYBION CID camera with a gating synchronized with the pulsing of the laser. For these measurements, the gating time was less than 1 μs and the camera was operated in a non-interlaced mode. Data were recorded through an interference filter with a full width half-maximum (FWHM) of 10 nm centered at 308 nm, allowing detection primarily from the (0,0) band. The camera resolution of 512 × 512 pixels allowed an average image resolution of 0.09 mm/pixel. Output of the camera was fed to a video recorder for continuous acquisition.

The videotaped data were digitized on a Macintosh II using a model DT2255 Data Translation digitizing card with a 640 × 480 square pixel format and associated image processing software. Images were digitized to 8-bits and the dynamic range was on the order of 30; however, the precise value of the signal to noise ratio varied from pixel to

TABLE I

Basic flow parameters with scaling estimates. Nozzle Reynolds number, Re = 2400. Nozzle exit velocity, U_{nozzle} = 108 m/s. Nozzle diameter, d = 2.5mm. Centerline velocity at a downstream distance x was estimated by $U_c = 6.4(d/x)U_{nozzle}$. The centerline rms velocity fluctuation, $u\prime \sim 0.3U_c$. Integral scale, L $\sim$ 0.25 local jet diameter. Turbulent Reynolds number, $Re_t = u\prime L/\upsilon$, where υ is the viscosity of hydrogen at 300K. Kolmogorov scale, $\eta = L(Re_t)^{\frac{-3}{4}}$. Damköhler number, $Da = \tau_f/\tau_c$, where τ_f = mixing time scale $= \eta^2/\upsilon$ and τ_c = reaction time scale. The latter was estimated to be 20 μs for 2-body forward reactions and 3 ms for 3-body recombination reactions (Barlow et al. 1990).

x/d	U_c(m/s)	u$\prime$(m/s)	L(mm)	Re_t	η(mm)	τ_f(μsec)	Da_{2-body}	Da_{3-body}
38	18.18	5.45	7.4	368	0.09	73	3.65	0.024
58	11.92	3.57	11.5	368	0.14	176	8.82	0.058
98	7.05	2.11	19.4	368	0.23	476	23.82	0.159

pixel, being the lowest where the structures were diffuse and OH concentrations low. The measurements here were limited to assessing the relative thickness of the spatial distribution of the OH regions, and the absolute value of pixel intensities and their relation to OH concentration were used only to determine the 'edges' of OH regions. Considering the system as a whole, the projected resolution amounts to approximately 0.095 mm/pixel in the vertical direction and 0.15 mm/pixel in the horizontal direction over a 46 mm × 46 mm area. The smallest structure measured was on the order of 1mm in width.

Twenty randomly selected images of the flame at each of the three streamwise locations were digitized. The thickness of the OH region in each of these images was measured at equal intervals along the length of the flame. At each interval, the shortest line across the OH region was defined and a profile of the pixel intensities along the line was obtained. The edge of the OH region was identified by setting a threshold of pixel intensity from which best defined the width of the profile and was sufficiently above the noise level of the image. The number of pixels along the line crossing the OH regions with intensities above the threshold value were then counted. This procedure was repeated using three different pixel intensity thresholds, corresponding to intensities 60, 70 and 80 percent below the maximum intensity. From visual observations, it was found that much lower thresholds would have been contaminated by noise. For comparison, hand measurements were also taken directly from images projected on to a large screen. In this technique the edges of the OH regions were determined visually rather than by pixel thresholding. It should be noted that glancing cuts of the laser through the jet add uncertainties to the interpretation of the data. Structures from the images which were clearly deemed as glancing cuts were not used in the analysis. From the recorded data, histograms of the thickness of the OH regions were produced.

3. RESULTS AND DISCUSSION

The basic parameters of the cold flow, estimated according to the 'standard' evolution of round jets (e.g., Wygnanski & Fiedler, 1968), are shown in Table I. These data are not directly relevant to the local flame front because the latter is nearly laminarized by the large heat release. Yet, the local reaction regions are buffeted by the turbulence in the core of the flow; some idea of the cold flow data was therefore thought to be appropriate. The turbulent Reynolds number Re_t is based on the estimated root-mean-square (rms) centerline velocity and integral scales. The Kolmogorov length and velocity scales, estimated according to the standard turbulence scaling relationship, are included; so are estimates of Damköhler number, Da, based on chemical reaction time scales of both the forward and recombination reactions.

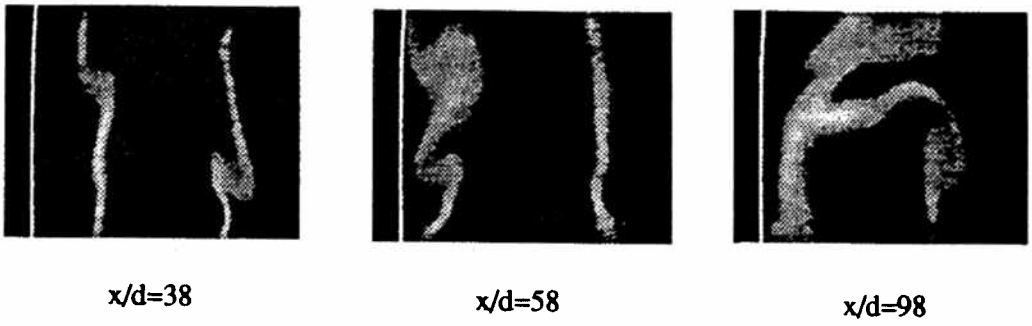

FIGURE 2. Visualizations of OH concentration in a hydrogen diffusion flame at three locations downstream of the nozzle. Reynolds number at the nozzle is Re = 2400. Nozzle diameter, d = 2.5 mm. Width of the images is x ~ 46 mm in real space.

Before we present the results, a comment is in order on the effect of buoyancy, which might be expected to have increasing influence with increasing distances from the nozzle. Some symptoms of buoyancy in jet flows include increases in momentum flux, Reynolds number, and activity and size of large eddies. In studies of buoyancy effects on turbulent diffusion flames of propane, Becker & Yamazaki (1978) found that transition from a momentum driven to a buoyant driven state begins when a nondimensional streamwise coordinate, $\xi = \mathrm{Ri}_s^{1/3}(\mathrm{x/D}_s)$, approaches a value between 1 and 2. Here, Ri_s is a 'source' Richardson number based on an effective 'source diameter' given by D_s. The value of ξ is substantially smaller in our flame except at the last measuring station, where it is of the order of 3. Thus, *a priori* considerations suggest that some effect of buoyancy may be present at the last measuring station. We shall later take a closer look at this issue.

Figure 2 shows three typical realizations of the OH regions at the three downstream positions mentioned earlier. As expected, they become more convoluted with increasing downstream distance. The OH regions are thin in comparison with the flow width, but their thickness is far larger than the Kolmogorov scale of the cold flow. As observed in a similar experiment on a hydrogen-air diffusion flame (Kychakoff et al., 1984), this relative fatness of the OH regions is in part due to the low Reynolds number of the flow. In the experiment by Kychakoff et al. (1984) it was found that with increasing Reynolds number, the width of the structures became smaller and had greater variations in size. Similar characteristics were also observed by Seitzman et al. (1990), who note that the diffuse structures are predicted well by the quasi-equilibrium distributed reaction (QEDR) model developed by Bilger (1988). A detailed review of the influence of other factors such as dissipation, mixture fraction and their role in the structure and thickness of turbulent nonpremixed flames can be found in Bilger (1988).

Because of the relatively slow recombination time of OH, we also expect the thickness of the OH regions to be broader than the instantaneous reaction zones. Bilger (1989a) gives an estimate for the flame thickness Λ in terms of the Kolmogorov scale η for one-step, second order irreversible reactions as $\Lambda/\eta = Da^{-1/3}Re^{1/4}Sc^{-1/2}\gamma\prime^{-1/3}$ where Sc is the Schmidt number and $\gamma\prime$ is the rms of mixture fraction. This relationship qualitatively explains how the Damköhler number can affect the size of a reaction zone. As shown in Table I, for hydrogen-air reactions Da is much smaller for the reverse reaction involving the free radical OH than for the forward reaction. Hence we expect OH regions to cover a larger area than the instantaneous flame region. For laminar counterflow methane-air diffusion flames, predicted number densities of both CH and OH in mixture fraction

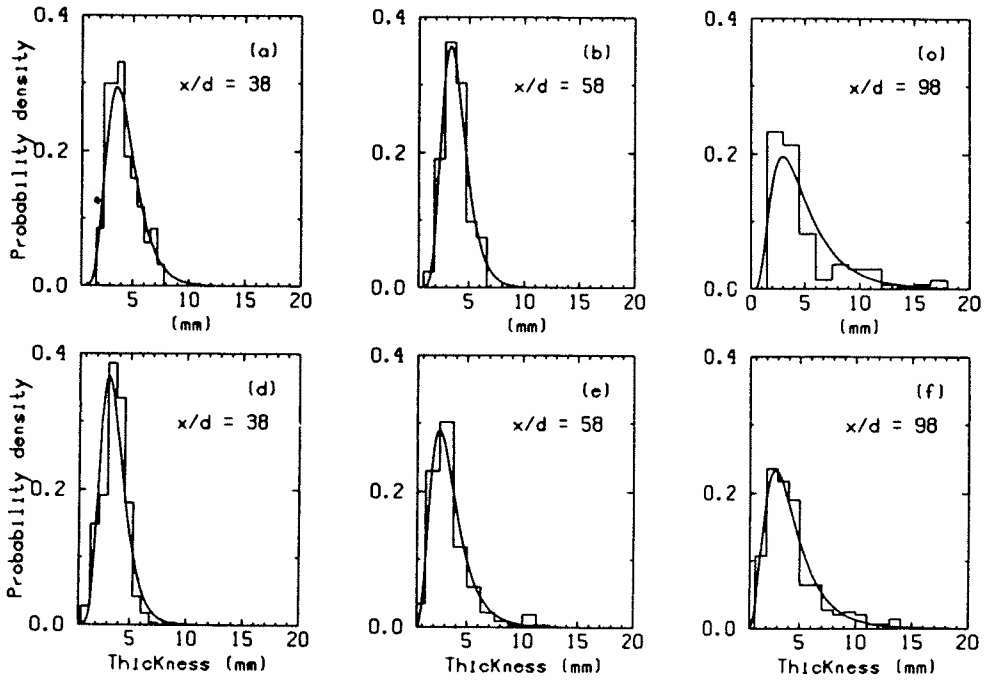

FIGURE 3. Distributions of the thickness of the OH regions at 38, 58, and 98 diameters downstream of the nozzle. (a)-(c): Edges of OH regions determined by setting a threshold on the pixel intensity (see text for details). (d)-(f): Edges of OH regions determined visually. Smooth curves denote fits using mean and rms values from the measurements.

space (Bilger, 1989b) have shown that the OH regions are broader and exist in high concentrations slightly to the lean side of the instantaneous reaction zone marked by CH.

Figures 3(a)-3(f) are histograms of the thickness of OH regions taken from the digitized images at 38, 58 and 98 diameters downstream. Figures 3(a)-3(c) represent measurements obtained by defining the 'edges' of the OH regions by a threshold which is 60% below the largest intensity. It was found that the histograms were the same for two other pixel thresholds (70% and 80% below the maximum intensity). Figures 3(d)-3(f) correspond to hand measurements described earlier. The histograms at each axial location, obtained by the two different methods, are reasonably close to each other. To the extent that the histograms are not sensitively dependent on the axial location, we infer that the buoyancy effects even at the last station are not severe—even though *a priori* considerations suggest otherwise. This should not come as a total surprise because buoyancy has different degrees of effect on different quantities; apparently, the normalized histograms belong to the category where the effects of moderate levels of buoyancy are minimal.

An attempt was made to fit the histograms with a lognormal probability density function using the measured mean and standard deviation. The lognormal fits, shown by the solid curves, are reasonable. The histograms were also fitted by the Rayleigh distribution function which is similar in shape to the lognormal. The Rayleigh distribution fits the body of the histograms reasonably well, but not the tails. It was found that the lognormal estimates were closer to the measurements. Low-order statistical data are presented in Table II.

TABLE II
Statistical averages from OH thickness measurements.

x/d	Average thickness (mm)	rms thickness (mm)	Skewness	Flatness
38	4.40	1.78	1.26	5.07
58	4.32	1.79	1.33	6.77
98	5.22	3.59	1.98	7.11

One would like to extend these statements to the reaction regions themselves. Unfortunately, as already remarked, because of the slow recombination time and temperature dependence of OH radicals, the visualized OH regions are larger than the reaction zone. The exact relationship between the thickness distribution of instantaneous and post combustion regions is not evident. However, OH has previously been noted as a good diagnostic of reaction zone structures (Hanson, 1987; Vandsburger et al., 1988; and Kychacoff et al., 1984). Experiments such as those by Smyth et al. (1985) on methane-air diffusion flames as well as the study of Bilger (1989b) and Keyes & Smooke (1990), have shown that peaks of OH concentrations coincide with high temperature areas and tend toward the lean side of the reaction zone. Although our reservations noted above remain in force, the prospect that these results are applicable to instantaneous flame and mixing regions is promising.

5. CONCLUSIONS

A hydrogen diffusion flame was visualized by the laser induced fluorescence of OH radicals. Measurements showed that the thickness of OH-containing regions is approximately lognormal. Such findings may be applicable to the flame thickness and to mixing interfaces.

ACKNOWLEDGEMENTS

We thank Professor R. W. Bilger for his comments on an earlier draft. A careful reading by a referee improved the text. This research has been supported by the United Technologies Corporation and the Air Force Office of Scientific Research.

REFERENCES

Barlow, R.S., Dibble, R.W., Chen, J.-Y., and Lucht, R.P. (1990) Effect of Damköhler Number on Superequilibrium of OH Concentration in Turbulent Nonpremixed Jet Flames. *Combustion and Flame,* **82,** 235.

Becker, H. A., and Yamazaki, S. (1978) Entrainment, Momentum Flux and Temperature in Vertical Free Turbulent Diffusion Flames. *Combustion and Flame,* **33,** 123.

Bilger, R. W. (1988) The Structure of Turbulent Nonpremixed Flames. *Twenty-Second Symposium (International) on Combustion/The Combustion Institute.* p. 475.

Bilger, R. W. (1989a) Turbulent Diffusion Flames. *Ann. Rev. Fluid Mech.* **21:** 101-135.

Bilger, R. W. (1989b) Reaction Zone Structure in Turbulent Diffusion Flames. *Joint International Conference Australia/New Zealand & Japanese Sections/The Combustion Institute, University of Sydney.*

Hanson, R.K. (1986) Combustion Diagnostics: Planar Imaging Techniques. *Twenty-First Symposium (International) on Combustion/The Combustion Institute.* p. 1677.

Keyes, D. E., and Smooke, M. D. (1989) Numerical Solution of 2-D Axisymmetric Laminar Diffusion Flames. *Combustion Science and Technology,* **67,** p. 85.

Kychakoff, G., Howe, R. D., Hanson, R. K., Drake, M. C., Pitz, R. W., Lap, M., and Penney, C. M., (1984) Visualization of Turbulent Flame Fronts with Planar Laser-Induced Fluorescence. *Science,* **224,** 382.

LaRue, J. C., and Libby, P. A. (1974) Temperature and Intermittency in the Turbulent Wake of a Heated Cylinder. *Phys. Fluids,* **17,** p. 873.

Pfefferle, L. D., Griffin, T. A., and Winter, M. (1988) Planar laser-induced fluorescence of OH in a chemically reacting boundary layer. *Applied Optics,* **27,** p. 3197.

Seitzman, J. M., Üngüt, A., Paul, P. H., and Hanson, R. (1990) Imaging and Characterization of OH Structures in a Turbulent Nonpremixed Flame. *Twenty-Third Symposium (International) on Combustion/The Combustion Institute,* p. 637.

Smyth, K. C., Miller, J. H., Dorfmann, R. C., Mallard, W. G., and Santoro, R. J. (1985) Soot Inception in a Methane/Air Diffusion Flame as Characterized by Detailed Species Profiles. *Combustion and Flame* **62,** p. 157.

Sreenivasan, K. R., Ramshankar, R., and Meneveau, C. (1989) Mixing, Entrainment, and the Fractal Dimension of Surfaces in Turbulent Flows. *Proc. R. Soc. Lond.* **A421,** p. 79.

Vandsburger, U., Seitzman, J. M. and Hanson, R. K. (1988) Visualization Methods for the Study of Unsteady Nonpremixed Jet Flame Structure. *Combustion Science and Technology,* **59,** p. 455.

Wygnanski, I., Fiedler, H. (1969) Some Measurements of the Self-Preserving Jet. *J. Fluid Mech.* **38,** p. 577.